

Cr/C Lamellar Multilayer Grating in Conical Diffraction Mounting for Beam Splitter used in X-ray Free-electron Lasers

YUFEI FENG,^{1,6} LIANGLIANG DU,^{2,6} QIUSHI HUANG,^{1,*} ZHENGKUN LIU³,
ANDREY SOKOLOV,⁴ RUNZE QI,¹ XIAOWEI YANG,⁵ ZHONG ZHANG,¹ AND
ZHANSHAN WANG,^{1,*}

¹MOE Key Laboratory of Advanced Microstructural Materials, Institute of Precision Optical Engineering, School of Physics Science and Engineering, Tongji University, Shanghai 200092, China

²Institute of Fluid Physics, China Academy of Engineering Physics, Mianyang, Sichuan 621999, China

³National Synchrotron Radiation Laboratory, University of Science and Technology of China, Hefei, Anhui 230029, China

⁴Helmholtz-Zentrum Berlin für Materialien und Energie, BESSY-II, Albert-Einstein-Str. 15, 12489 Berlin, Germany

⁵Center for Transformative Science, ShanghaiTech University, 393 Middle Huaxia Road, Pudong, Shanghai, China

⁶These authors contributed equally: Yufei Feng, Liangliang Du.

*Corresponding author: huangqs@tongji.edu.cn; wangzs@tongji.edu.cn

Received XX Month XXXX; revised XX Month, XXXX; accepted XX Month XXXX; posted XX Month XXXX (Doc. ID XXXXX); published XX Month XXXX

A lamellar multilayer grating in a conical diffraction mounting was proposed as a beam splitter for X-ray free-electron lasers. Theoretical calculations demonstrated that the distribution of diffraction efficiency can be adjusted by optimizing the groove depth or d-spacing. A Cr/C multilayer lamellar grating with a line density of approximately 2500 L/mm was fabricated. The performance of the element was measured in the Optics Beamline PM-1 (BESSY-II) at an energy of 1500 eV. A five-order diffraction pattern was recognized, and the diffraction efficiency of the $-/+1^{\text{st}}$ order was approximately 12.6% and 4.4%, respectively. The asymmetric distribution of diffraction efficiency can be caused by the different sidewall angles of the grating groove. © 2021 Optical Society of America.

Radiation pulses from the X-ray free-electron laser (XFEL) have an unprecedented peak power (>10 GW) and an ultrashort temporal duration (<100 fs) [1-2]. Based on this, the electronic and structural dynamics of matter can be observed by the “Pump-probe” systems with angstrom and femtosecond resolution in spatial and temporal domains [3-4]. Meanwhile, most current XFEL sources are based on the self-amplified spontaneous emission (SASE) scheme, which causes variations in the properties of radiation pulses such as pulse energy, temporal duration, and wavefront [5]. The diagnostics of each incoming pulse are critical for the normalization and analysis of signals.

Split-and-delay optics (SDO) are essential for both “pump-probe” systems and photon-beam diagnostics [6]. Beam splitter, which divides XFEL pulses into double pulses or more, is located at the front of the system and is essential for the success of the experiment. Several types of beam splitters have been explored, including mirror-based splitters [7-8], transmission grating-based splitters [9-10], and ultrathin crystal-based splitters [11-12]. Mirror-based elements realize beam splitting using a special sharp edge, where

the small tolerance of angle deviation in mirror mounting makes it difficult to control [8]. Transmission gratings and ultrathin crystal-based components must use transmitted diffracted beams to achieve beam splitting, which is a huge challenge for element fabrication and has potential thermal stability issues [4].

An innovative lamellar grating based on conical diffraction has been proposed as a beam splitter [13]. In this case, the incident beam is parallel to the grating groove, and the diffraction beams are divided into several orders in the off-plane, as shown in Fig. 1. In particular, the diffraction pattern and efficiency are highly symmetric, and high efficiency can be achieved because of the reduced shadowing effect in a conical diffraction mounting [13]. In addition, the broadening duration of plus of conical diffraction mounting, which is determined by the number of illuminated grooves of grating, could be an order of magnitude smaller than that of classical diffraction mounting in grazing incidence mode [14]. Braig et al. [15] and Jark et al. [16] experimentally verified beam splitting using a single-layer lamellar grating with a conical diffraction mounting. However, because the incident beam is

working in the total reflection area, a large grating element has to be prepared to receive the entire beam footprint, and the system for introducing a certain time delay is large. Multilayer gratings, which have been developed as efficient monochromator by diffraction in in-plane mode [17-18], can operate at a much higher grazing incidence compared with single-layer gratings with a narrower bandwidth owing to the Bragg reflection principle. A higher incidence angle will also result in a larger time delay in a pump-probe system [19]. Therefore, a lamellar multilayer grating working in the conical diffraction mode can be used as an efficient, compact, and flexible X-ray beam splitter. Goray [20] theoretically investigated the diffraction performance of multilayer lamellar gratings in conical diffraction for approximately 12 keV X-rays. In this letter, the diffraction properties of multilayer lamellar gratings with a conical diffraction mounting are investigated, and the first experimental demonstration is presented.

In the conical diffraction configuration of a multilayer lamellar grating, the radiation beam is incident along the groove and the diffracted beam lies along an arc on a cone, as shown in Fig. 1. The incident beam can be described by ϕ , which is the angle between the direction of the rays and one of the grooves, and θ , which is the angle representing the deviation of the plane of the rays and grooves from the plane of the groove and the surface normal. For the specific grating period p and wavelength λ , the diffraction equation of the m^{th} -order diffracted beam can be written as

$$p \sin \phi (\sin \theta + \sin \theta_m) = m \lambda. \quad (1)$$

where θ_m is the angle of diffracted beam.

For a more convenient operation in the experiment, the beam can be defined by two other parameters: γ , which is the angle between the direction of the ray and its projection in the plane of the grating surface, and η , which is the angle between the direction of the projection of rays on the grating surface and one of the grooves. The two sets of angles can be connected via a transformation.

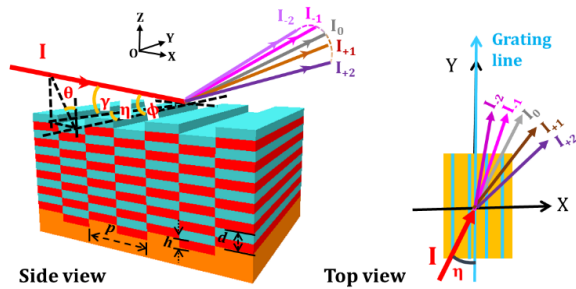


Fig. 1. Schematic view of the multilayer lamellar grating in a conical diffraction mounting, viewed from the side and top, respectively.

In the case of the multilayer grating, the angle γ and d-spacing must meet the multilayer Bragg diffraction conditions to obtain a high diffraction efficiency. Therefore, it is necessary to investigate the change in diffraction efficiency for different structures of multilayer lamellar gratings with a conical diffraction mounting.

For the first demonstration, considering tender X-rays ($E=1000\text{--}5000$ eV) as a typical working region for multilayer gratings where crystals are difficult to cover, Cr/C is an ideal multilayer to provide high reflectance in this range [21]. We calculated the conical diffraction of Cr/C multilayer lamellar gratings at energies of 1500 eV and 4500 eV, for which the grating

period was $p = 400$ nm (2500 L/mm), and the ratio of the groove to the period was set to 0.5. The d-spacing of the multilayers was maintained at 10 nm, and the diffraction efficiency as a function of incident angle γ , with $\eta = 0^\circ$, was calculated at different groove depths h . In this case, the peak position of the diffraction curve always appears at a fixed angle γ of approximately 2.68° for 1500 eV and 0.89° for 4500 eV, which is determined by the d-spacing of the multilayer. Fig. 2 presents the evolution of the diffraction efficiency with the change in the groove depth h . The results indicate that the diffraction efficiency shows a periodic variation, in the case of both 1500 and 4500 eV. The evolution of the diffraction efficiency of the $\pm 1^{\text{st}}$ orders is the same and is opposite to that of the zeroth order. Meanwhile, it can be observed that the maximum diffraction efficiency at different energies corresponds to the same groove depth. When the groove depth h is about 4.5 and 13.5 nm, the diffraction efficiency of the $\pm 1^{\text{st}}$ orders reaches maximum (about 19.3% for 1500 eV and 35.3% for 4500 eV), and the diffraction efficiency of the 0^{th} order reaches the maximum when $h = 9$ nm and $h = 18$ nm (about 45.1% for 1500 eV and 84.7% for 4500 eV). It should be pointed out that the diffraction efficiency in the article is absolute efficiency, i.e. diffracted intensity normalized by the incident intensity for the multilayer grating. In addition, there is a groove depth ($h = 6.12$ nm) at which the same diffraction efficiency is achieved (approximately 12.5% for 1500 eV and 24.7% for 4500 eV) for the 0^{th} and $\pm 1^{\text{st}}$ orders, which is convenient for developing a multichannel beam splitter. The change in efficiency could be caused by the different interference effects of the reflections from the land and the groove surfaces of the multilayer. The optical path difference between these two parts is equal to $2hs \sin \gamma$ for the reflection plane, that is, the position of the 0^{th} order. When the optical path difference equals λ , the constructive interference in the reflection plane contributes to the maximum diffraction efficiency of the 0^{th} order. When the optical path difference equals $\pm \lambda/2$, the diffraction efficiency of the $\pm 1^{\text{st}}$ orders reaches the maximum value. In other words, a special efficiency ratio between different orders can be obtained by optimizing the groove depth. In this study, a groove depth of 4.5 nm was selected to obtain the highest efficiency of the $\pm 1^{\text{st}}$ order, while completely suppressing the zeroth order.

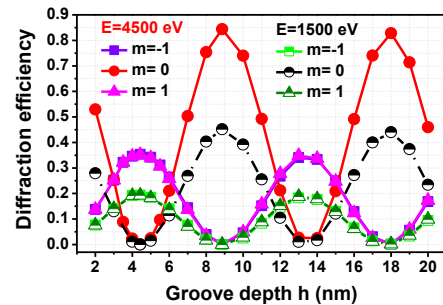


Fig. 2. The evolution of the diffraction efficiency of the 0^{th} , $\pm 1^{\text{st}}$ orders of a Cr/C multilayer lamellar grating with a conical diffraction mounting for a change of groove depth h at energies of 1500 eV and 4500 eV.

The grating substrates were fabricated at the University of Science and Technology of China, Hefei, and the actual grating groove depth was approximately 5.5 nm with a period of approximately 400 nm (2500 L/mm) based on the AFM results. The multilayer parameters must be optimized to match the grating structure. We calculated the diffraction curves as a function of

incident angle γ , while $\eta = 0^\circ$, with different d-spacings of multilayers, and recorded the maximum diffraction efficiency of the 1st order in each case. Fig. 3 shows the evolution of the diffraction efficiency with the change in the d-spacing of the multilayer at energies of 1500 eV and 4500 eV. The results showed the same evolution trend at different energy values. The change was also caused by the interference of the reflections from the land and the groove surfaces of the multilayer grating. In the case of $d = 6.12$ nm, the incident angles are approximately 4.30° for 1500 eV and 1.43° for 4500 eV, and the optical path difference equals λ , which maximizes the diffraction efficiency of the 0th order. It is worth noting that, in the case of large d-spacing (approximately 10–18 nm), the diffraction efficiency of the $\pm 1^{\text{st}}$ orders changed slower with the increase in d-spacing, in contrast to the case of small d-spacing, which can be explained by the slower variation of the optical path difference as the incident angles became smaller. This large tolerance was beneficial to the experimental fabrication. As the d-spacing continued to increase, the optical path difference gradually decreased to zero, resulting in an increase in the diffraction efficiency of the 0th order. We selected the case of $d = 11.5$ nm for the experimental demonstration, in which the splitting angles $\Delta\theta = \theta_1 - \theta_{-1}$ were approximately 16.92° and 5.64° ($\Delta\eta = 0.23^\circ/0.08^\circ$), and the diffraction efficiencies were approximately 18.5% and 35.4%, at the energies of 1500 eV and 4500 eV, respectively.

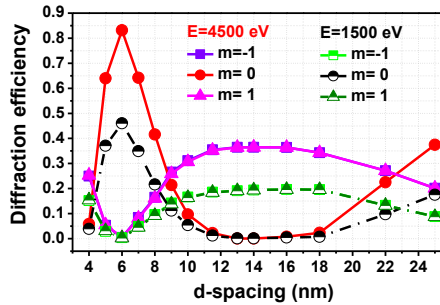


Fig. 3. The evolution of the diffraction efficiency of the 0th, $\pm 1^{\text{st}}$ orders of a Cr/C multilayer lamellar grating with a conical diffraction mounting for a change of d-spacing of multilayer at energies of 1500 eV and 4500 eV.

The Cr/C multilayer gratings and their reference multilayer mirror samples were fabricated using a direct-current magnetron sputtering technique. Based on our previous optimization of deposition [22], the samples were deposited at an Ar gas pressure of 3 mTorr at room temperature, and the background pressure was lower than 9.0×10^{-5} Pa. The d-spacing of the Cr/C multilayer is 11.5 nm, the ratio of the Cr layer thickness to the total thickness was 0.4, and the saturated layer number was 10. The structure of the multilayers was characterized by grazing incidence X-ray reflection (GIXRR), and the groove shape of the multilayer gratings was characterized using atomic force microscopy (AFM). Fig. 4 presents the AFM image of the groove profile of the Cr/C multilayer grating; the grating structure is clear and regular. The reference Cr/C multilayer samples were also measured by AFM, and the surface RMS roughness was about 0.21 nm.

To verify the beam splitting property of the multilayer lamellar gratings in the conical diffraction mounting, the optical performance of the sample was preliminarily measured with Optics Beamline PM-1 at the BESSY-II facility at an energy point of approximately 1500 eV. The sample structure was aligned

individually with high accuracy in six degrees of freedom [22].

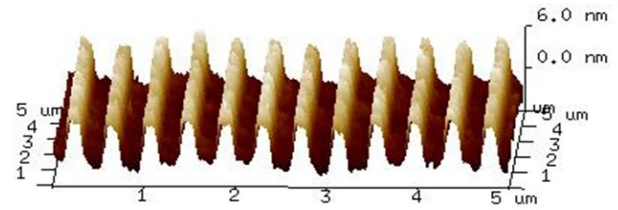


Fig. 4. The AFM image of the groove profile of the lamellar grating after coating with the Cr/C multilayer.

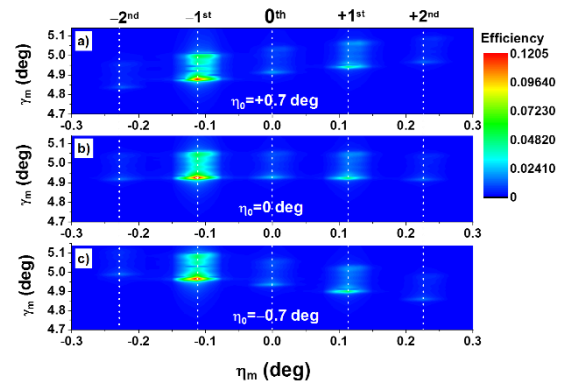


Fig. 5. The diffraction patterns of the Cr/C multilayer grating in the conical diffraction mounting with incident angle γ_0 of about 2.48° and different η_0 . a) $\eta_0 = +0.7^\circ$; b) $\eta_0 = 0^\circ$; c) $\eta_0 = -0.7^\circ$.

We found the highest diffraction efficiency of the -1^{st} order at an incident angle γ_0 of approximately 2.48° , while the incident beam was parallel to the groove, that is, $\eta_0 = 0^\circ$. Fig. 5(b) presents the diffraction pattern of the Cr/C multilayer grating with a conical diffraction mounting. The five-order diffraction pattern is symmetrically distributed in a slight arc. The diffraction patterns were recorded when the incident beam was deflected from the groove direction by $\pm 0.7^\circ$, that is, $\eta_0 = \pm 0.7^\circ$, as shown in Fig. 5(a) and 5(c), respectively. The diffraction patterns were deflected, as expected, because of the deflection of the incident beam. The peak positions of the diffraction orders were matched with the calculated results, in which the structural parameters of the multilayer grating were obtained by AFM and GIXRR measurements. The results demonstrated the feasibility of the beam splitting of multilayer lamellar gratings with a conical diffraction mounting.

The measured diffraction efficiency of the Cr/C multilayer lamellar grating in the conical diffraction mounting is shown in Fig. 6. The efficiency of the -1^{st} order is approximately 12.6%, which is significantly larger than that of the $+1^{\text{st}}$ order (approximately 4.4%). The calculated diffraction efficiency of the ideal lamellar groove model is also presented in Fig. 6, in which the efficiencies of the $\pm 1^{\text{st}}$ orders are the same. We found that the distribution of the diffraction efficiency of the multilayer lamellar grating in the conical diffraction mounting was controlled by the groove shape. In our case, the asymmetric sidewalls ($\alpha_1 = 3.4^\circ$ and $\alpha_2 = 11.2^\circ$) could be observed from the measured AFM profile, shown in the upper right corner of Fig. 6. The diffraction efficiency can be calculated by setting up a grating with an asymmetrical groove shape. The results

showed that the asymmetry in diffraction efficiency with $\alpha_1 = 3^\circ$ and $\alpha_2 = 15^\circ$ is close to the measured efficiency trend. The results indicate that the asymmetric distribution of efficiency can be caused by the different angles of the sidewalls of the grating grooves.

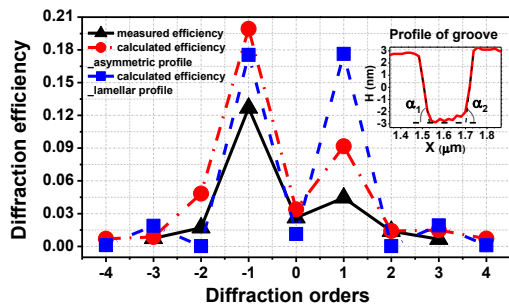


Fig. 6. The measured and calculated distribution of diffraction efficiency of the Cr/C multilayer lamellar grating in the conical diffraction mounting. The insert in the upper right of Figure is the groove profile from the AFM results.

The diffraction efficiency of the Cr/C multilayer lamellar grating with a conical diffraction mounting was measured as a function of photon energy near 1500 eV. At each energy point, the incident angle of γ_0 was fixed at 2.48° , and the incident angle of η_0 was maintained at 0° . The diffraction patterns were recorded by rotating the detector with an aperture of $0.4 \times 4 \text{ mm}^2$. The integral efficiency, which summed the intensity of the aperture, of each energy point was calculated and is presented in Fig. 7. At the same time, as a comparison, the calculated diffraction efficiency curves as a function of energy were also presented in the figure. For better analysis and comparison, the calculated efficiency values were normalized so that the calculated efficiency of the -1^{st} order was the same as the measured efficiency at an energy of 1500 eV. The variation trend of the measured efficiency with energy in the conical diffraction mounting is the same as the calculated one. The lower experimental efficiency can be caused by the asymmetry of the groove shape and imperfect multilayer structure.

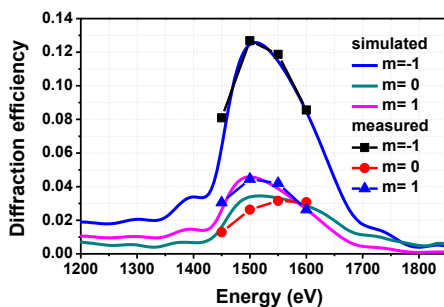


Fig. 7. The measured and calculated evolution of diffraction efficiency of the Cr/C multilayer lamellar grating in the conical diffraction mounting as a function of energy.

In summary, we theoretically designed a lamellar multilayer grating in a conical diffraction mounting for the tender X-ray region and experimentally demonstrated its diffraction and beam splitting properties for the first time. The calculated results indicate that the efficiency ratio of different orders can be flexibly adjusted by optimizing the groove depth and d-spacing, which has great

potential for the development of multichannel beam splitters. The measured results proved that a five-order diffraction pattern could be recognized, and the efficiencies of the $-/+1^{\text{st}}$ orders were approximately 12.6% and 4.4%, respectively. The distribution of the efficiency was affected by the angles of the sidewalls of the grating groove. This work can provide important guidance for the development of lamellar multilayer gratings in conical diffraction mounting for beam splitters of XFEL. The conical diffraction of multilayer gratings also has great potential for X-ray astronomical spectroscopy with high resolution and high efficiency [23].

Funding. National Natural Science Foundation of China (12075170, 11805189, U1732268, 11805127) and Shanghai Rising-Star Program (No. 19QA1409200).

Disclosures. The authors declare no conflicts of interest.

Data availability. No data were generated or analyzed in the presented research.

References

1. P. Emma, R. Akre, J. Arthur, R. Bionta and C. Bostedt., *Nat. Photonics* **4**, 64 (2010).
2. H. Tanaka and M. Yabashi, *Nat. Photonics* **6**, 540 (2012).
3. M. C. Newton, M. Sao, Y. Fujisawa, R. Onitsuka and T. Kawaguchi, *Opt. Express* **18**, 17620 (2010).
4. J. R. Rouxel, D. Fainozzi, R. Mankowsky, B. Rösner and G. Seniutinas, *Nat. Photonics* **15**, 499 (2021).
5. E. L. Saldin, E. A. Schneidmiller and M. V. Yurkov, *New J. Phys.* **12**, 035010 (2010).
6. W. Roseker, H. Franz, H. Schulte-Schrepping, A. Ehnes and O. Leupold, *Opt. Lett.* **34**, 1768 (2009).
7. S. Roling, S. Braun, P. Gawlitza, M. Wöstmann and E. Ziegler, *Opt. Lett.* **39**, 2782 (2014).
8. S. Roling, H. Zacharias, L. Samoylova, H. Sinn and T. Tschentscher, *Phys. Rev. ST Accel. Beams* **17**, 110705 (2014).
9. C. David, P. Karvinen, M. Sikorski, S. Song and I. Vartiainen, *Sci. Rep.* **5**, 1 (2015).
10. T. Katayama, S. Owada, T. Togashi, K. Ogawa, P. Karvinen and I. Vartiainen, *Struct. Dyn.* **3**, 034301 (2016).
11. T. Osaka, T. Hirano, Y. Sano, Y. Inubushi and S. Matsuyama, *Opt. Express* **24**, 9187 (2016).
12. Y. P. Stetsko, Y. V. Shvyd'ko, and G. B. Stephenson, *Appl. Phys. Lett.* **103**, 173508 (2013).
13. W. Jark and D. Eichert, *J. Synchrotron Rad.* **23**, 91 (2016).
14. F. Frassetto, C. Cacho, C. A. Froud, I. C. Turcu, P. Villorosi, W. A. Bryan, E. Springate, and L. Poletto, *Opt. express* **19**, 20 (2011).
15. C. Braig, L. Fritzsche, T. Käsebieber, E.-B. Kley and C. Laubis, *Opt. Express* **20**, 1825 (2012).
16. W. Jark and D. Eichert, *Opt. Express* **23**, 22753 (2015).
17. D. L. Voronov, E. M. Gullikson, F. Salmassi, T. Warwick, and H. A. Padmore, *Opt. Lett.* **39**, 11 (2014).
18. R. van der Meer, I.V. Kozhevnikov, H.M.J. Bastiaens, K.-J. Boller, and F. Bijkerk, *Opt. Express* **21**, 11 (2013).
19. S. Roling, V. Kärcher, L. Samoylova, *Proc. of SPIE Vol. 10237* (2017).
20. L. I. Goray, *Journal of Surface Investigation. X-ray, Synchrotron and Neutron Techniques* **2**, 796 (2008).
21. A. Sokolov, Q. Huang, F. Senf, J. Feng and S. Lemke, *Opt. Express* **27**, 12 (2019).
22. Y. Feng, Q. Huang, Y. Zhuang, A. Sokolov and S. Lemke, *Opt. Express* **29**, 13416 (2021).
23. J. H. Tutt, R. L. McEntaffer, H. Marlowe, D. M. Miles and T. J. Peterson, *Instrum.* **5**, 3 (2016).